Stem Cell Reports
Report
OPEN ACCESS

Purification and Ex Vivo Expansion of Fully Functional Salivary Gland Stem Cells

Lalitha S.Y. Nanduri,[1] Mirjam Baanstra,[1,2] Hette Faber,[1,2] Cecilia Rocchi,[1,2] Erik Zwart,[3] Gerald de Haan,[3] Ronald van Os,[3] and Robert P. Coppes[1,2,*]

[1]Department of Cell Biology, University Medical Center Groningen, University of Groningen, Antonius Deusinglaan 1, 9713AV Groningen, the Netherlands
[2]Department of Radiation Oncology, University Medical Center Groningen, University of Groningen, Hanzeplein 1, 9713GZ Groningen, the Netherlands
[3]Laboratory of Ageing Biology and Stem Cells, European Research Institute for the Biology of Aging (ERIBA), University Medical Center Groningen, University of Groningen, Building 3226, Antonius Deusinglaan 1, 9713AV Groningen, the Netherlands
*Correspondence: r.p.coppes@umcg.nl
http://dx.doi.org/10.1016/j.stemcr.2014.09.015

SUMMARY

Hyposalivation often leads to irreversible and untreatable xerostomia. Salivary gland (SG) stem cell therapy is an attractive putative option to salvage these patients but is impeded by the limited availability of adult human tissue. Here, using murine SG cells, we demonstrate single-cell self-renewal, differentiation, enrichment of SG stem cells, and robust in vitro expansion. Dependent on stem cell marker expression, SG sphere-derived single cells could be differentiated in vitro into distinct lobular or ductal/lobular organoids, suggestive of progenitor or stem cell potency. Expanded cells were able to form miniglands/organoids containing multiple SG cell lineages. Expansion of these multipotent cells through serial passaging resulted in selection of a cell population, homogenous for stem cell marker expression ($CD24^{hi}/CD29^{hi}$). Cells highly expressing CD24 and CD29 could be prospectively isolated and were able to efficiently restore radiation-damaged SG function. Our approach will facilitate the use of adult SG stem cells for a variety of scientific and therapeutic purposes.

INTRODUCTION

Saliva, the secretion of the salivary gland (SG), crucially maintains the physiological balance in the oral cavity and initiates food digestion. Like many other organs, SGs undergo cell renewal, presumably enforced by a small pool of stem cells. Dysfunctional SG homeostasis may be caused by improper SG stem cell functioning, leading to disease. Disease-induced hyposalivation often leads to xerostomia, with symptoms including dry mouth/nasal passages, sore throat, loss of oral hygiene, dental caries, oral candidiasis, loss of taste, and difficulties with swallowing and speaking, which collectively reduce the patient's quality of life (Vissink et al., 2010). Hyposalivation can be a consequence of autoimmune disorders (Sjögren syndrome), endocrine disorders (diabetes mellitus and hyper-/hypothyroidism), neurologic disorders, or radiation damage in head and neck cancer patients after radiotherapy.

Treatment options for xerostomia include administration of saliva substitutes or stimulants (Fox, 2004). Saliva substitutes might improve some, but not all, problems associated with SG dysfunction, whereas stimulants are only useful for people with some remaining SG function. Alternative approaches to restore SG function have been pursued, for instance, the development of bioengineered glands (Ogawa et al., 2013). Although this may be a good model to study SG regeneration, it might not be clinically translatable due to its origin from embryonic SGs. Another potential option is to rescue these patients using autologous stem cell transplantation that may regenerate the damaged tissue and thus provide long-term recovery.

It has been shown that ductal ligation induced damage to the SG-stimulated proliferation of CD29- and CD49f-expressing cells (Matsumoto et al., 2007), indicating the existence of regenerative cells in this area of the SG. We reported earlier that murine (Lombaert et al., 2008) and human (Feng et al., 2009) stem/progenitor cells can be cultured into salispheres (primary spheres) via an enrichment culture in vitro. In preclinical models, we demonstrated the potential of autologous adult stem cell transplantation to restore radiation-damaged SG function (Lombaert et al., 2008; Nanduri et al., 2011) and tissue homeostasis (Nanduri et al., 2013). Murine SG primary-sphere-derived $c\text{-}KIT^{+}$ cells were able to restore SG function in hyposalivation mouse model. Unfortunately, scarce adult human biopsy material contains very low numbers of $c\text{-}KIT^{+}$ cells (Feng et al., 2009; Pringle et al., 2013), limiting their clinical potential. An alternative strategy is therefore necessary to generate sufficient stem/progenitor cells numbers to enable translation of this therapy to the clinic.

Expanding the number of stem cells ex vivo represents a way to circumvent this problem. In contrast to induced pluripotent stem cells and embryonic stem cells, adult stem cells are not easily propagated and expanded. Self-renewal/expansion has been reported for only a few types of adult stem cells, including neural (Kalani et al., 2008), intestinal (Barker et al., 2007), and liver stem cells (Huch

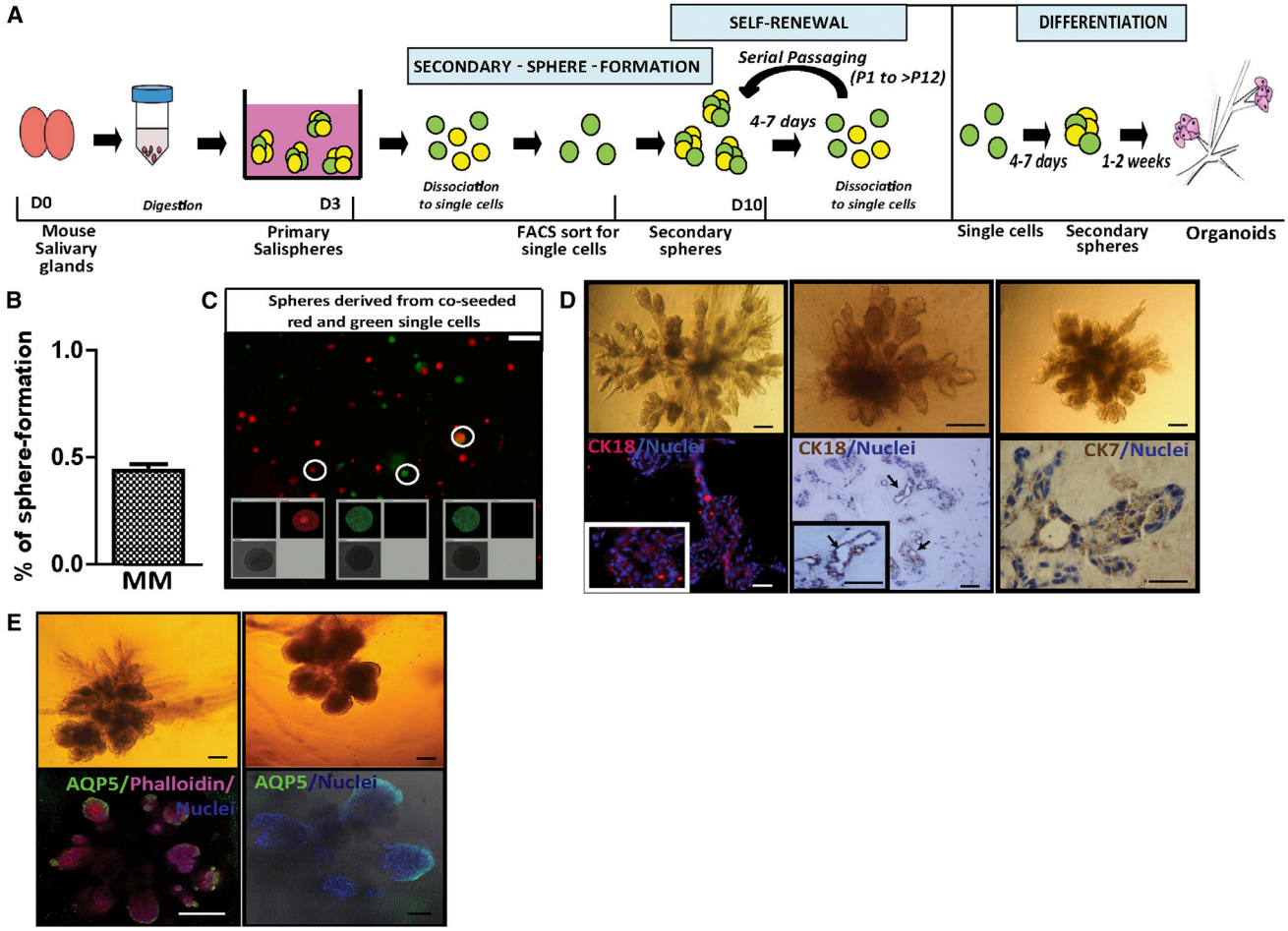

Figure 1. Self-Renewal and Differentiation Potential Salisphere-Derived Cells

(A) Diagrammatic representation of primary-sphere culture from enzymatically digested murine SG, followed by steps for secondary-sphere formation, self-renewal by continuous replating, and differentiation assays in Matrigel/collagen.

(B) Percentage sphere formation of primary-sphere-derived unselected cells in minimal medium (MM) (n = 5 independent experiments); error bars are SEM.

(C) Image showing predominantly (99.2%) single-cell-derived spheres from murine DsRed and GFP SG cells in coculture; scale bar, 50 μm.

(D) Photomicrographs of organoid formation in differentiation cultures showing ductal organoids stained positive for cytokeratin18 and cytokeratin7 SG duct markers; scale bar, 50 μm.

(E) Lobular organoids positive for aquaporin5, an acinar cell marker (scale bar, 50 μm).

et al., 2013), but the long-term functional activity of these cultured cells remains to be assessed.

Therefore, the aim of the current study is to investigate the expansion potential of fully functional murine SG stem cells.

RESULTS

First, in vitro assays were used to test self-renewal and differentiation properties of primary spheres, being a putative stem or progenitor cell population. To test their self-renewal ability, murine primary-sphere-derived single cells were fluorescence-activated cell sorting sorted and seeded into a Matrigel-based matrix (10,000 cells/gel) supplemented with minimal culture medium (MM) (see the Experimental Procedures; Figure 1A). Within 5–7 days 0.44% ± 0.03% of the single cells formed secondary spheres (Figure 1B, MM). When primary-sphere-derived single cells from DsRed and enhanced GFP (EGFP) transgenic mice were mixed and coseeded, more than 99% of all secondary spheres were single colored (Figure 1C), indicating that the spheres are not formed by clumping of cells, but rather through the outgrowth from single cells.

To test the ability of putative SG stem cells to differentiate into mature cell lineages, single-cell-derived spheres

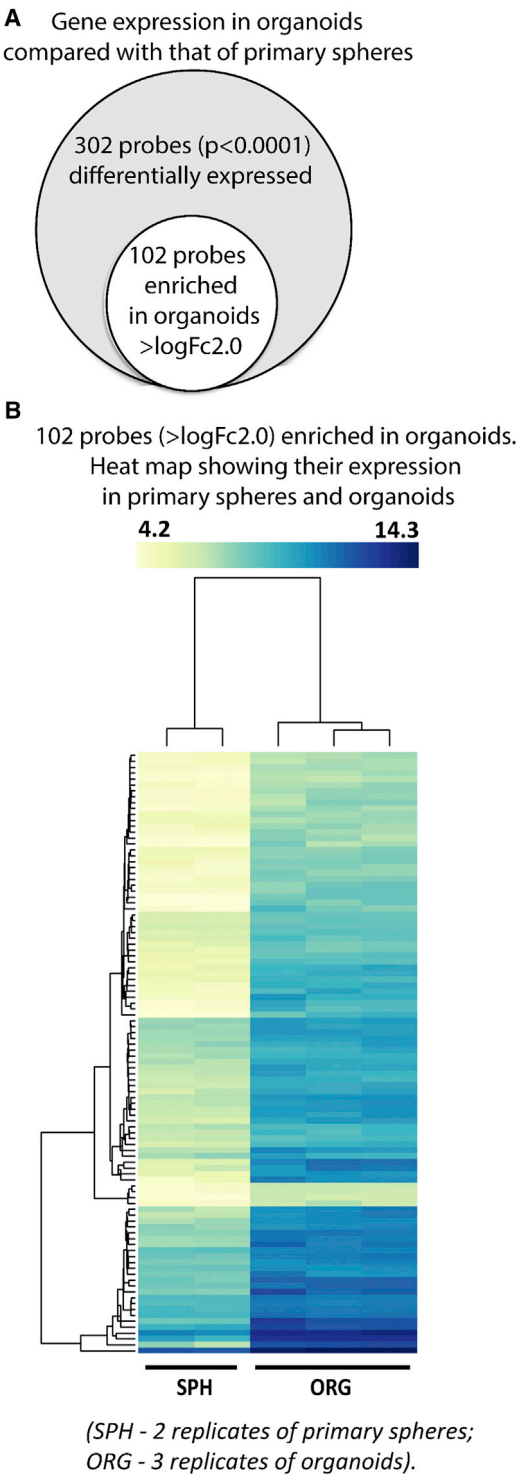

Figure 2. Gene Expression Analysis of State of Differentiation in Organoids

(A) Venn diagram showing 102 differentially expressed probes enriched in organoids (samples from n = 3 independent experiments) compared to undifferentiated primary spheres (samples from n = 3 independent experiments).

(B) Heatmap showing expression of genes (minimum 4.2 to maximum 14.5) in organoids (ORG) and primary spheres (SPH) that are involved in gene ontology annotations as described in the manuscript.

See also Tables S1 and S2.

were plated into a 3D matrix mixture of collagen and Matrigel, supplemented with minimal medium with 10% fetal calf serum (Figure 1A, Differentiation). Within 1–3 weeks, the seeded spheres changed morphologically into diverse organoid-like structures. Two types of organoids, ductal and lobular, could be discerned. Ductal organoids contained a lumen (arrows) and were surrounded by cells that stained positive for CK7 and CK18 (Figure 1D), which is consistently expressed in SG duct cells. The lobular organoids were devoid of tubular extensions but rather contained compact, round, lobule-like structures, which expressed the acinar cell protein aquaporin-5 (Figure 1E, AQP5). To confirm genome-wide signs of differentiation in the organoids, a gene expression analysis was performed (details in the Experimental Procedures; Gene Expression Omnibus [GEO] accession number GSE59559). Data from organoids were compared to that of primary spheres (representing a relatively undifferentiated state) using differential gene expression analysis. Results identified 302 differentially expressed probes in organoids when compared to primary spheres (Figure 2A) with a stringent threshold ($p < 0.0001$). Among these, 102 probes were upregulated (>logFc2.0) in organoids (Figure 2B) compared to primary spheres (Table S1 available online). They were tested for gene ontology classifiers that revealed significant enrichment in biological processes including gland morphogenesis (GO: 0022612), gland development (GO: 0048732), and many others listed in Table S2. At the individual gene level, these 102 genes include calcium-channel-related proteins (CPNE8), secretin (role in pancreatic duct secretion; Lee et al., 2012); cranio-facial-development-related RBMS3 gene (Jayasena and Bronner, 2012), vitamin-K-dependent protein (PROS1), vesicle-associated membrane protein (VAMP4; Sramkova et al., 2012), STRA6 (Petrakova et al., 2014) known to be expressed in SG, SG-branching morphogenesis-related (TGM2 and NTN4), and embryonic SG end bud differentiation marker (fibroblast growth factor 1; Patel et al., 2006), indicating SG-specific differentiation. These findings show that single-cell-derived spheres are capable of secondary sphere formation, which can form differentiated SG lineages in vitro.

Studies from other glandular tissues, like mammary gland, revealed $CD24^{hi}/CD29^{lo}$- (Shackleton et al., 2006) expressing cells as potential stem cells. In mice, we reported that intraglandular transplantation of primary-sphere-derived $CD24^{+}/CD29^{+}$ cells could ameliorate

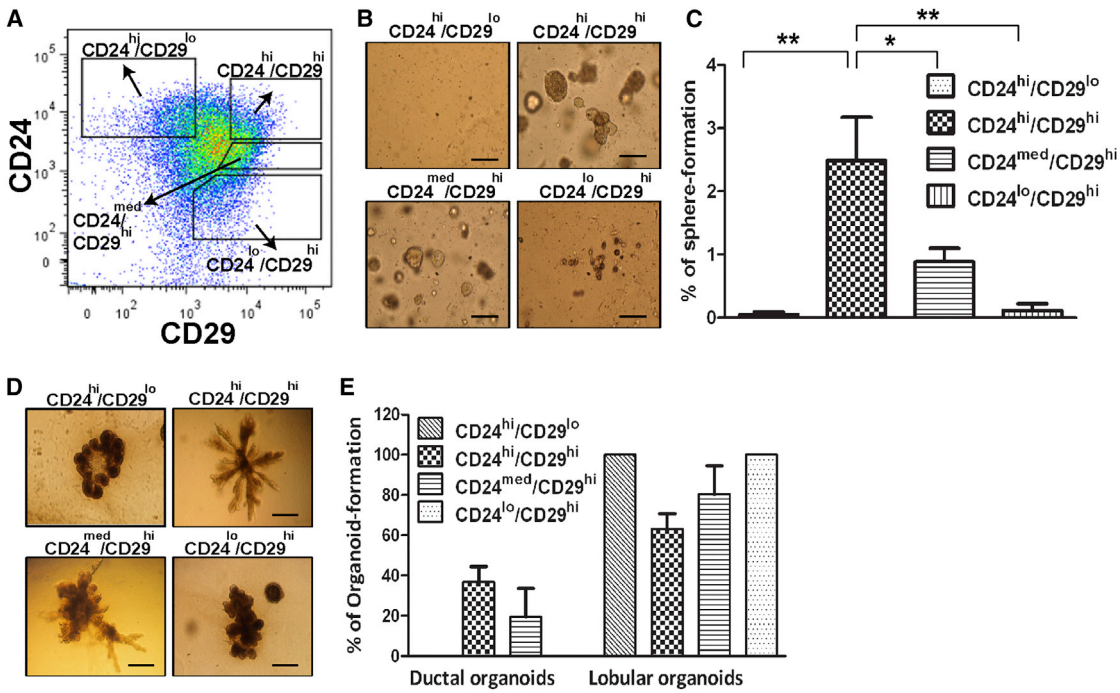

Figure 3. Self-Renewal and Differentiation Potential of Subsets of CD24/CD29-Expressing Cells

(A) Flow cytometric gating strategy used to separate CD24- and CD29-stained primary-sphere-derived cells into four subsets: $CD24^{hi}/CD29^{lo}$; $CD24^{hi}/CD29^{hi}$; $CD24^{med}/CD29^{hi}$; and $CD24^{lo}/CD29^{hi}$.

(B) Photomicrographs showing single-cell-derived secondary spheres in culture (end of P1) from all the four CD24/CD29 subsets; scale bar, 50 μm.

(C) Percentage secondary sphere forming of the various CD24/CD29 subsets (one-way ANOVA; *$p < 0.05$; **$p < 0.01$; ***$p < 0.001$) with five biological replicates each. Error bars are SEM.

(D) Photomicrograph of single-cell-derived organoids from four CD24/CD29 subsets in vitro (scale bar, 50 μm).

(E) Percentage of spheres from CD24/CD29 subsets that form ductal- or lobular-type organoids from n = 3 independent experiments. Organoids from $CD24^{hi}/CD29^{hi}$ cells constitute 36.7% ± 4.3% of ductal organoids and 63.1% ± 4.3% of lobular organoids, whereas from $CD24^{med}/CD29^{hi}$ cells constitute 19.5% ± 8.1% of ductal organoids and 80.4% ± 8.1% of lobular organoids. All the organoids from $CD24^{lo}/CD29^{lo}$ cells and $CD24^{hi}/CD29^{lo}$ cells are lobular organoids. Error bars are SEM.

See also Figure S1.

radiation-induced hyposalivation to some extent (Nanduri et al., 2011).

Therefore, we next tested whether subpopulations exist in primary-sphere-derived single cells (Figure 1A) that express CD24 and/or CD29 using flow cytometry. Unlike the situation in the mammary gland (Shackleton et al., 2006), we did not detect a clear separation between subsets. Therefore, the cells were arbitrarily separated into four subsets ($CD24^{hi}/CD29^{lo}$, $CD24^{hi}/CD29^{hi}$, $CD24^{med}/CD29^{hi}$, and $CD24^{lo}/CD29^{hi}$) using the gating strategy shown in Figure 3A. Sorted single cells were plated into MM culture medium. After 5–7 days, secondary spheres were formed from all subsets (Figure 3B), albeit with different efficiencies. Clearly, the $CD24^{hi}/CD29^{hi}$ cells showed the highest secondary-sphere-formation capacity (Figure 3C).

Next, these secondary spheres were induced to form organoids. Although all four subsets formed organoids, these were morphologically very distinct (Figure 3D). Detailed analysis of the different types of organoids showed that $CD24^{hi}/CD29^{hi}$ and $CD24^{med}/CD29^{hi}$ cells have the ability to form both ductal and lobular organoids whereas $CD24^{hi}/CD29^{lo}$ and $CD24^{lo}/CD29^{hi}$ cells form predominantly lobular organoids (Figure 3E), most likely implying a more committed cell state in the latter two populations.

To assess their self-renewal potential, cells from all populations were cultured under MM conditions. Most cells from $CD24^{hi}/CD29^{lo}$ and $CD24^{lo}/CD29^{hi}$ subsets do not proliferate or die during culture as observed with trypan-blue-based cell counting. Very few form secondary spheres that did not yield enough cells to allow passaging. $CD24^{med}/CD29^{hi}$- and $CD24^{hi}/CD29^{hi}$-derived cells, however, were able to self-renew for four passages and greater than five passages, respectively (Figure S1A), indicating the higher potential of these populations. During

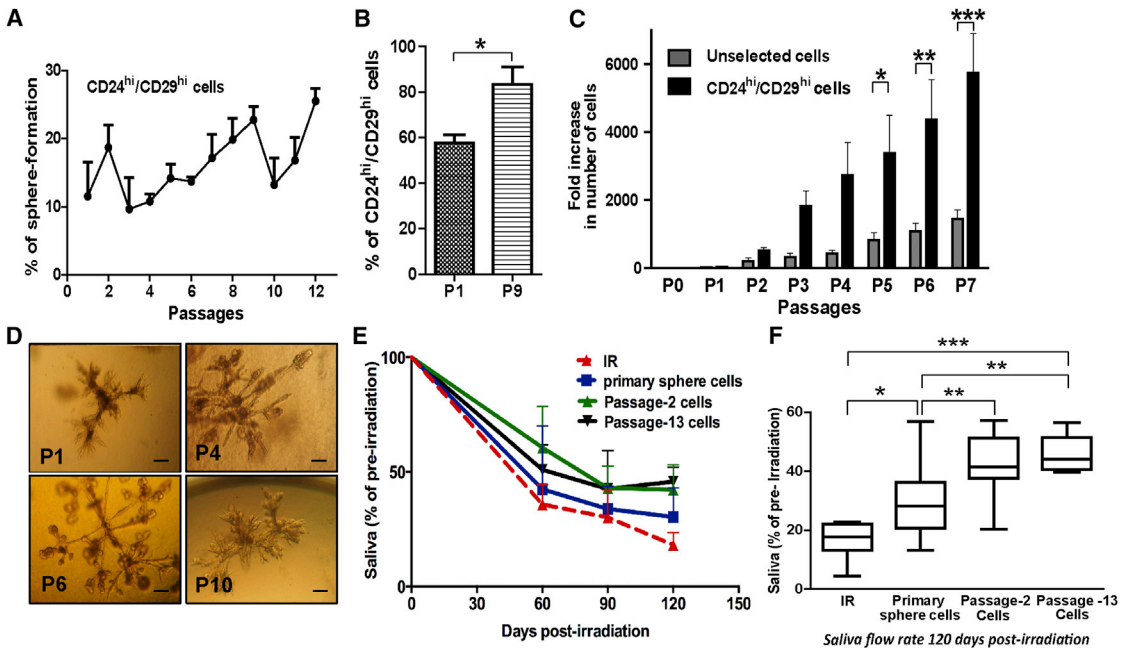

Figure 4. Potency of Expanded Salisphere-Derived CD24^{hi}/CD29^{hi} Cells

(A) Percentage sphere formation related to the number of passages (x axis) of CD24^{hi}/CD29^{hi} cells from n = 4 independent experiments. Error bars are SEM.

(B) Increase ($p < 0.05$) in percentage of CD24^{hi}/CD29^{hi} cells determined by flow cytometry in self-renewal passage 1 (P1) and P9 from n = 4 independent experiments. Error bars are SEM.

(C) Expansion of CD24^{hi}/CD29^{hi} and unselected cells at different passages in self-renewal conditions (two-way ANOVA; *$p < 0.05$; **$p < 0.01$; ***$p < 0.001$). Data from n = 4 independent experiments. Error bars are SEM.

(D) Photomicrograph showing single-cell-derived ductal organoids from expanded cells at various passages (P1, P4, P6, and P11); scale bar, 50 μm.

(E) Graph showing saliva (% of preirradiation; y axis) at different days postirradiation from the irradiated, nontransplanted mice and mice transplanted with different cell populations.

(F) The box-whisker plot shows recovery of saliva (as % of preirradiation values) in irradiated (15 Gy) mice 90 days posttransplantation with primary-sphere-derived CD24^{hi}/CD29^{hi} cells, passage 2, or passage 13 cells in comparison to irradiated, nontransplanted controls (n = 6–10 mice/group). Note the uniform response in all mice transplanted with passage 13 cells. (*$p < 0.01$; **$p < 0.001$; ***$p < 0.001$; one-way ANOVA). All error bars are SEM.

See also Figures S1–S3 and Tables S3 and S4.

self-renewal, spheres are dissociated to single cells at every passage. To minimize dissociation-induced stress, the Rho-inhibitor Y-27632, known to protect against dissociation-induced cell stress, was added (Zhang et al., 2011; enriched medium [EM]). It enhanced the initial secondary sphere-formation percentage of CD24^{hi}/CD29^{hi} cells (Figure S1B) from 2.5% ± 0.68% (MM) to 10.9% ± 3.9% (EM). Next, CD24^{hi}/CD29^{hi} cells were cultured under EM conditions, which resulted in a more-rapid and pronounced expansion of cells capable of forming secondary spheres. In general, the percentage of cells capable of forming spheres was increased with increasing passages (Figure 4A) from 11.54% ± 5.02% at passage 1 (P1) to 25.51% ± 1.86% at P12 ($p < 0.05$; Figure S1C), indicative of enrichment for sphere-forming cells. This is further emphasized by the significant increase (Figure 4B) in cells expressing CD24^{hi}/CD29^{hi} from P1 to P9 (Figure S1D).

Compared to expansion from unselected cells, a striking 4-fold increased (5,734 ± 1,148 cells) number of CD24^{hi}/CD29^{hi} cells was generated after seven passages (Figure 4C). Thus, a pronounced expansion of apparent SG stem cells can be obtained with these optimized in vitro cultures. Such expansion may be a key element in the future therapeutic use of these cells to restore SG function in patients included in prolonged (multiple weeks) radiotherapy regimens (Vergeer et al., 2009).

Karyotyping of passaged sphere cells showed doubling of the number of chromosomes in about 50% of the cells that were cultured beyond passage 3 (data not shown), a phenomenon known to occur in mice (Tolar et al., 2007).

However, we have so far not seen any tumor formation after transplantation of these cells (see below).

To identify differentially regulated genes in long-term self-renewing SG cells, genome-wide gene expression analysis (GEO accession number GSE59559) was performed on primary-sphere-derived $CD24^{hi}/CD29^{hi}$ cells (P0) and $CD24^{hi}/CD29^{hi}$ cells that were passaged ten (P10) times. Gene-expression analysis with a stringent threshold of $p < 0.0001$ has identified 229 probes that are differentially expressed between P0 and P10 $CD24^{hi}/CD29^{hi}$ cells (Figure S1E). Among these, 13 genes were upregulated (>logFc 4.0) in P10 compared to P0 cells, indicating their enrichment during later passages (Table S3). These include *CCD3*, *PORCN*, *CAV1*, *SNCG*, *TRP63*, *CCND2*, *KRT5*, *LGALS7*, *SNAI2*, *NTRK2*, *GPR87*, *VSNL1*, and *DST* (Figure S1F).

Pathway analysis on these genes identified their role in stem-cell-maintenance-related Wnt pathway (Baker, 2010), cell-cycle-related p53 pathway, JAK stat, and MAPK pathways in addition to others listed in Table S4. These results suggest a potential contribution of multiple signaling pathways for stem cell maintenance during long-term self-renewal culture. However, extensive studies are needed to elucidate the exact role of these regulator genes/pathways for the SGs.

To test whether these expanded long-term self-renewing cells retain SG identity, spheres at passages 1, 4, 6, and 11 were subjected to differentiation conditions, which resulted in formation of ductal/lobular organoids (Figure 4D), indicating their multipotent character. These results show that $CD24^{hi}/CD29^{hi}$ cells have the ability to self-renew, expand, and differentiate into SG lineages in vitro. Our assays thus offer an opportunity to preselect potential stem cell populations, which reduce the time and number of animals needed for in vivo testing.

Finally, we tested the potential of these cells to rescue radiation-induced hyposalivation in vivo. $CD24^{hi}/CD29^{hi}/EGFP^{+}$ SG-derived primary spheres, passage 2 spheres, or passage 13 spheres were transplanted into locally 15 Gy X-rays-irradiated submandibular glands (5,000/gland) 30 days after irradiation. Saliva flow of all transplanted and irradiated, nontransplanted mice was measured at 60, 90, and 120 days postirradiation and represented as percentage of preirradiation saliva (Figure 4E). Pilocarpine-stimulated SG function improved in all treated groups. Interestingly, mice transplanted with expanded cells recovered saliva flow to 46% ± 2.11% of preirradiation values, which is extraordinary as only two (submandibular glands) out of six (submandibular, parotid, and sublingual glands) irradiated glands were transplanted. The recovery after transplantation of passage 13 cells was more uniform (Figure 4F) in comparison to all other groups, indicative of a more-homogenous cell population. Recovery of glandular tissue was demonstrated by the improvement of general morphology (Figure S2A; hematoxylin and eosin) and reappearance of functional acinar tissue that is characterized by aquaporin-5 acinar cell marker expression (Figure S2B; aquaporin5). The histological improvement was more apparent in mice transplanted with expanded SG stem cells when compared to irradiated and resembled the histology of nonirradiated controls. Extensive formation of donor-derived $EGFP^{+}$ acinar cells was observed in recipient tissue (Figure S2C), demonstrating the functional contribution of donor cells to the gland. Though expanded cells showed abnormal chromosomal number, we did not observe any tumor formation in all the transplanted mice. Together, these data reveal that purification of $CD24^{hi}/CD29^{hi}$ SG stem cells and culturing them in self-renewal conditions extensively expands stem cells with pronounced potential to restore functionality in destroyed submandibular glands. However, the contribution of endogenous stem cells for the recovery cannot be excluded, e.g., through stimulation with factors secreted by the transplanted cells.

In previous studies, we showed that primary-sphere-derived $c\text{-}KIT^{+}$ (Lombaert et al., 2008) or $c\text{-}KIT^{+}/CD24^{+}/CD49f^{+}$ triple-positive cells (Nanduri et al., 2011, 2013) could rescue functionality of radiation-damaged SGs. Therefore, we analyzed the expression of $c\text{-}KIT^{+}$ cells within the $CD24^{hi}/CD29^{hi}$ subpopulation (Figure S3A). Data show that all $c\text{-}KIT^{+}$ cells are contained within the subpopulation of the $CD24^{hi}/CD29^{hi}$, whereas very few $c\text{-}KIT^{+}$ cells overlap with $CD49f^{+}/CD24^{+}$ double-positive population (Figure S3A). Next, we tested whether $c\text{-}KIT^{+}$ or $c\text{-}KIT^{-}$ cells within the $CD24^{hi}/CD29^{hi}$ population are responsible for regeneration in our in vivo model. Transplantation of primary-sphere-derived $c\text{-}KIT^{+}/CD24^{+}/CD29^{+}$ and $c\text{-}KIT^{-}/CD24^{+}/CD29^{+}$ or the $c\text{-}KIT^{+}/CD24^{+}/CD49f^{+}$ triple-positive population induced at best a similar recovery of salivary flow (Figure S3B) when compared to the total $CD24^{hi}/CD29^{hi}$ population. This indicates that enrichment of $c\text{-}KIT^{+}$ cells within the $CD24^{+}/CD29^{+}$ does not further enrich for stem cells within the $CD24^{hi}/CD29^{hi}$ population capable of regenerating irradiated glands.

DISCUSSION

In this study, we demonstrated the long-term in vitro maintenance and expansion of primary-sphere-derived $CD24^{hi}/CD29^{hi}$ cells. These cells retained their ability to self-renew and remained fully functional upon transplantation. In addition to our in vivo experiments, we have developed various short-term in vitro assays that were instrumental in characterizing the potency of candidate stem cell

populations. Unlike mammary glands (Shackleton et al., 2006), we did not observe separate subsets of CD24/CD29-expressing cells in primary spheres using flow cytometry. However, the in vitro sphere formation and self-renewal assays did distinguish distinct subsets of CD24/CD29-expressing cells. Different subsets had distinct self-renewal capacities, with the $CD24^{hi}/CD29^{hi}$ having the highest potency. Similarly, in the organoid-formation assay, the different subsets lead to morphologically distinct structures. The $CD24^{lo}/CD29^{hi}$ and $CD24^{hi}/CD29^{lo}$ populations formed more lobular organoids, suggestive of more committed progenitor cells. On the other hand, $CD24^{hi}/CD29^{hi}$ and $CD24^{med}/CD29^{hi}$ cells formed both ductal and lobular organoids and may therefore have more multipotent, stem-cell-like properties. These conclusions are in agreement with our in vivo data where $CD24^{hi}/CD29^{hi}$ cells provided efficient regeneration of irradiated SGs. The availability of these solid in vitro assays will allow screening of putative stem cell populations for their differentiation and self-renewal capacity.

Most importantly, the successful expansion and enrichment of SG stem/progenitor cells as shown in this study are auxiliary and prerequisite for the translation and establishment of stem cell therapy for patients with hyposalivation.

EXPERIMENTAL PROCEDURES

Sphere Culture

Mouse SGs were mechanically and enzymatically digested and cultured into primary spheres. For flow cytometric analysis of stem cell marker expression, primary spheres were made into single cells using trypsin and stained with CD24, CD29, c-KIT, and CD49f antibodies. For details regarding protocols, see the Supplemental Experimental Procedures.

In Vitro Self-Renewal

Primary-sphere-derived single unselected cells or cells from CD24/CD29 subsets were cultured in Matrigel and incubated with self-renewal medium for secondary-sphere formation. To test long-term self-renewing potential, secondary spheres are made into single cells and replated for the next passage, and this procedure is repeated at the end of every passage. For details regarding protocols, see the Supplemental Experimental Procedures.

In Vitro Organoid Formation

To test organoid-forming ability of spheres, secondary spheres at the end of any/some passages in self-renewal were collected and placed in Matrigel:collagen matrix supplemented with differentiation medium. Spheres are observed every 2 or 3 days for organoid formation. To identify the different cell types in the organoids, they are stained with salivary-gland-cells-specific markers like aquaporin5, cytokeratin7, etc. and imaged with confocal imaging. For details regarding protocols, see the Supplemental Experimental Procedures.

Irradiation and Transplantation

To induce hyposalivation, mouse SGs are locally irradiated with 15 Gy (Precision X-Ray X-RAD 320, 200 kV, 20 mA, and 1.843 Gy/min). Thirty days postirradiation, primary-sphere-derived cells were sorted for $CD24^{hi}/CD29^{hi}$, or dissociated cells from passage 2 and passage 13 spheres were transplanted intraglandular into the irradiated mouse SGs. Saliva is collected pre- and postirradiation and transplantation as a functional readout of transplantation. For details regarding protocols, see the Supplemental Experimental Procedures.

Microarray Expression Profiling and Analysis

Highly pure total RNA (300 ng/sample) was extracted from all the samples used in the array using QIAGEN RNAeasy micro kit and used for expression profiling on Illumina WG-6 v2.0 expression bead chip kit. The data were normalized using the R version 3.0.1 *neqc* function of the BioConductor version 2.12 library *limma 3.16.5* (Smyth et al., 2005) by control background correction, quantile normalization and log2 transformation, and batch effects between arrays. Differential expression analysis was performed using *eBayes* function of the BioConductor library *limma* and an adjustment method Benjamini Hochberg was used with a p value of 0.05. Gene Ontology analysis was performed using Amigo labs (http://amigo1.geneontology.org/cgi-bin/amigo/term_enrichment). Heatmaps were made by R library heatmap.plus 1.3 and RcolorBrewe 1.0-5.

ACCESSION NUMBERS

Microarray data deposited in GEO database can be accessed with the GEO accession number GSE59559.

SUPPLEMENTAL INFORMATION

Supplemental Information includes Supplemental Experimental Procedures, three figures, and four tables and can be found with this article online at http://dx.doi.org/10.1016/j.stemcr.2014.09.015.

ACKNOWLEDGMENTS

We thank L.V. Bystrykh for his valuable advice on microarray analysis, B.N. Giepmans for collaboration with microscopy facility, and K. Borgmann for chromosome analysis. We would like to acknowledge The Netherlands Organization for Health Research and Development (ZonMW; grant no. 11.600.1023), the Dutch government to the Netherlands Institute for Regenerative Medicine (NIRM; grant no. FES0908), and Dutch Cancer Society (RUG2008-4022) for financial support of this project. Part of this work has been performed at the UMCG Microscopy and Imaging Center (UMIC), which is sponsored by NWO grant no. 175-10-2009-023.

Received: January 19, 2014
Revised: September 22, 2014
Accepted: September 23, 2014
Published: October 23, 2014

REFERENCES

Baker, O.J. (2010). Tight junctions in salivary epithelium. J. Biomed. Biotechnol. *2010*, 278948.

Barker, N., van Es, J.H., Kuipers, J., Kujala, P., van den Born, M., Cozijnsen, M., Haegebarth, A., Korving, J., Begthel, H., Peters, P.J., and Clevers, H. (2007). Identification of stem cells in small intestine and colon by marker gene Lgr5. Nature *449*, 1003–1007.

Feng, J., van der Zwaag, M., Stokman, M.A., van Os, R., and Coppes, R.P. (2009). Isolation and characterization of human salivary gland cells for stem cell transplantation to reduce radiation-induced hyposalivation. Radiother. Oncol. *92*, 466–471.

Fox, P.C. (2004). Salivary enhancement therapies. Caries Res. *38*, 241–246.

Huch, M., Dorrell, C., Boj, S.F., van Es, J.H., Li, V.S., van de Wetering, M., Sato, T., Hamer, K., Sasaki, N., Finegold, M.J., et al. (2013). In vitro expansion of single Lgr5+ liver stem cells induced by Wnt-driven regeneration. Nature *494*, 247–250.

Jayasena, C.S., and Bronner, M.E. (2012). Rbms3 functions in craniofacial development by posttranscriptionally modulating TGF-β signaling. J. Cell Biol. *199*, 453–466.

Kalani, M.Y., Cheshier, S.H., Cord, B.J., Bababeygy, S.R., Vogel, H., Weissman, I.L., Palmer, T.D., and Nusse, R. (2008). Wnt-mediated self-renewal of neural stem/progenitor cells. Proc. Natl. Acad. Sci. USA *105*, 16970–16975.

Lee, M.G., Ohana, E., Park, H.W., Yang, D., and Muallem, S. (2012). Molecular mechanism of pancreatic and salivary gland fluid and HCO3 secretion. Physiol. Rev. *92*, 39–74.

Lombaert, I.M., Brunsting, J.F., Wierenga, P.K., Faber, H., Stokman, M.A., Kok, T., Visser, W.H., Kampinga, H.H., de Haan, G., and Coppes, R.P. (2008). Rescue of salivary gland function after stem cell transplantation in irradiated glands. PLoS ONE *3*, e2063.

Matsumoto, S., Okumura, K., Ogata, A., Hisatomi, Y., Sato, A., Hattori, K., Matsumoto, M., Kaji, Y., Takahashi, M., Yamamoto, T., et al. (2007). Isolation of tissue progenitor cells from duct-ligated salivary glands of swine. Cloning Stem Cells *9*, 176–190.

Nanduri, L.S., Maimets, M., Pringle, S.A., van der Zwaag, M., van Os, R.P., and Coppes, R.P. (2011). Regeneration of irradiated salivary glands with stem cell marker expressing cells. Radiother. Oncol. *99*, 367–372.

Nanduri, L.S., Lombaert, I.M., van der Zwaag, M., Faber, H., Brunsting, J.F., van Os, R.P., and Coppes, R.P. (2013). Salisphere derived c-Kit cell transplantation restores tissue homeostasis in irradiated salivary gland. Radiother. Oncol. *108*, 458–463.

Ogawa, M., Oshima, M., Imamura, A., Sekine, Y., Ishida, K., Yamashita, K., Nakajima, K., Hirayama, M., Tachikawa, T., and Tsuji, T. (2013). Functional salivary gland regeneration by transplantation of a bioengineered organ germ. Nat. Commun. *4*, 2498.

Patel, V.N., Rebustini, I.T., and Hoffman, M.P. (2006). Salivary gland branching morphogenesis. Differentiation *74*, 349–364.

Petrakova, O.S., Terskikh, V.V., Chernioglo, E.S., Ashapkin, V.V., Bragin, E.Y., Shtratnikova, V.Y., Gvazava, I.G., Sukhanov, Y.V., and Vasiliev, A.V. (2014). Comparative analysis reveals similarities between cultured submandibular salivary gland cells and liver progenitor cells. Springerplus *3*, 183.

Pringle, S., Van Os, R., and Coppes, R.P. (2013). Concise review: Adult salivary gland stem cells and a potential therapy for xerostomia. Stem Cells *31*, 613–619.

Shackleton, M., Vaillant, F., Simpson, K.J., Stingl, J., Smyth, G.K., Asselin-Labat, M.L., Wu, L., Lindeman, G.J., and Visvader, J.E. (2006). Generation of a functional mammary gland from a single stem cell. Nature *439*, 84–88.

Smyth, G.K., Michaud, J., and Scott, H.S. (2005). Use of within-array replicate spots for assessing differential expression in microarray experiments. Bioinformatics *21*, 2067–2075.

Sramkova, M., Masedunskas, A., and Weigert, R. (2012). Plasmid DNA is internalized from the apical plasma membrane of the salivary gland epithelium in live animals. Histochem. Cell Biol. *138*, 201–213.

Tolar, J., Nauta, A.J., Osborn, M.J., Panoskaltsis Mortari, A., McElmurry, R.T., Bell, S., Xia, L., Zhou, N., Riddle, M., Schroeder, T.M., et al. (2007). Sarcoma derived from cultured mesenchymal stem cells. Stem Cells *25*, 371–379.

Vergeer, M.R., Doornaert, P.A., Rietveld, D.H., Leemans, C.R., Slotman, B.J., and Langendijk, J.A. (2009). Intensity-modulated radiotherapy reduces radiation-induced morbidity and improves health-related quality of life: results of a nonrandomized prospective study using a standardized follow-up program. Int. J. Radiat. Oncol. Biol. Phys. *74*, 1–8.

Vissink, A., Mitchell, J.B., Baum, B.J., Limesand, K.H., Jensen, S.B., Fox, P.C., Elting, L.S., Langendijk, J.A., Coppes, R.P., and Reyland, M.E. (2010). Clinical management of salivary gland hypofunction and xerostomia in head-and-neck cancer patients: successes and barriers. Int. J. Radiat. Oncol. Biol. Phys. *78*, 983–991.

Zhang, L., Valdez, J.M., Zhang, B., Wei, L., Chang, J., and Xin, L. (2011). ROCK inhibitor Y-27632 suppresses dissociation-induced apoptosis of murine prostate stem/progenitor cells and increases their cloning efficiency. PLoS ONE *6*, e18271.